

Numerical Investigation of Thermal-hydraulic Phenomena in a Full-scale Fuel Assembly

Gi-Uk Choi^a, Sun-Rock Choi^b, Min-Seop Song^{c*}, Jae-Ho Jeong^{a*}

^aGachon University, 1342, Seongnam-daero, Sujeong-gu, Seongnam-si, Gyeonggi-do

^bKorea Atomic Energy Research Institute, 111 Daedeok-daero, 989 Beon-gil, Yuseong-gu, Daejeon 34057

^cDepartment of Nuclear Engineering, Seoul National University, 559 Gwanak-ro, Gwanak-gu, Seoul

*Corresponding author: jaeho.jeong@gachon.ac.kr

1. Introduction

The Korea Atomic Energy Research Institute's Prototype Gen-IV Sodium-cooled Fast Reactor (PGSFR) is a reactor that uses fast neutrons to generate fission reactions and transfers heat using sodium as a coolant. SFR (Sodium-cooled Fast Reactor) has attracted a lot of attention from several countries as a solution to the problem of sustainable energy supply, because it is compact and has high power density.

The high thermal energy generated in the fuel by nuclear fission could lead to material damage due to the thermal stresses created in the clad when significant temperature changes are subjected around its circumference. [1] Therefore, it is important to accurately predict the velocity and temperature profile of the coolant in the fuel assembly. In addition, determining the peak cladding temperature, hotspot location, and temperature gradient in hexagonal duct are important for design and safety analysis decisions. [2]

The temperature of the cladding and coolant of the nuclear fuel assembly in the core are investigated in order to meet the safety tolerance standards. Therefore, the core thermal design of the SFR must ensure adequate fuel thermodynamic performance. [3]

Many previous studies have been conducted in order to investigate the thermal-hydraulic behavior of nuclear fuel assemblies, using various turbulence models of computational fluid dynamic (CFD) [4-6]. However, very few studies investigate the thermal behavior of fuel assemblies at full scale using the SST turbulence model.

In the present study, the thermal and hydraulic behavior of a real scale 217-pin wire-wrapped fuel assembly of KAERI-PGSFR are investigated with RANS based CFD methodology. [4]

The RANS-based CFD analysis with normal operating power distribution was performed ANSYS CFX code.

The friction factor and Nusselt number at various Reynolds number ranges were verified with correlation equations. In addition, three-dimensional thermal-hydraulic behavior were investigated to elucidate the thermo-hydraulic behavior in the 217-pin wire wrap fuel assembly in a steady state of nuclear power plant.

2. Numerical Method

2.1 Computational grid system

Fig. 1 shows the computational grid configuration of the PGSFR 217PIN fuel assembly, it is composed of 50 million Hexahedron elements. An innovative grid generation method using Fortran-based in-house code

was applied [7]. Because the actual wire shape is simulated without distortion of the shape, the prediction of the contact area between the wire and the rod can be made more accurately. Simulation results using this methodology have been proven that it is possible to accurately predict the pressure drop and flow analysis of the nuclear fuel assembly [4].

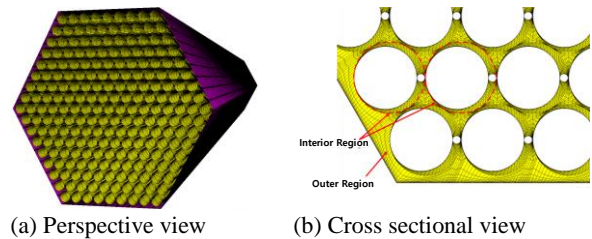


Fig. 1. Computational grid system of the fuel assembly

2.2 CFD Modeling

PGSFR 217-pin wire-wrapped fuel assembly was designed by the Korea Atomic Energy Research Institute (KAERI) in 2014 [8]. The core of PGSFR is loaded with metal fuels of U-Zr and generates a nuclear heat of 392.2 MWt. The major design parameters are summarized in Table 1. Fig. 2 shows the number of pins of the nuclear fuel assembly and the power distribution for each pin, and Fig. 3 shows the normalized axial power distribution. The power distribution has already been selected through the core design. Most of the heat output is generated in the region of the fuel assembly. The closer to the center of the core, the higher the heat output of the fuel assembly, so the power distribution is displayed differently for each pin. [9] CFD investigations in this study were performed on the heated region of a PGSFR 217 fin fuel assembly.

Table 1. Geometric information of fuel assembly

Geometry Parameters	Values
Number of pins	217
Pin diameter	7.4 mm
Clad thickness	0.5 mm
Wire diameter	0.95 mm
Wire lead pitch	221 mm
Pin pitch	8.436 mm
Total length	2.15 m
CFD computation length	1.1 m
Active length	0.98 m
Non-Heat length	0.12 m
Duct width	126.36 mm
Coolant	Sodium

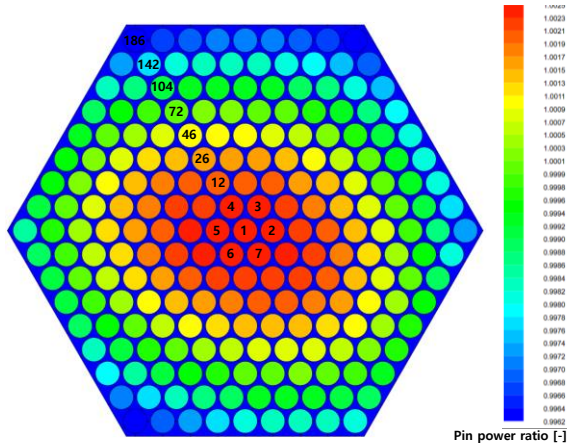


Fig. 2. Pin power distribution and Pin number position

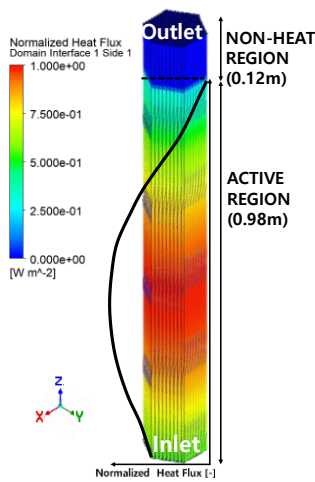


Fig. 3. Axial heat flux distribution

2.3 Boundary condition

Table 2. describes the boundary conditions for CFD analysis. The inlet is defined as a mass flow rate of various values and the outlet is defined as a constant outlet pressure of 3.5 bar. After the total power was uniformly applied to 217 pins, the distribution was applied as shown in Fig. 2 and 3. Eq. (1) is the boundary condition expression of heat flux for each pin.

$$\sum_{i=1}^{217} P(\text{pin}_i) * P(z) * Q_{avg} = \text{Total Power [kW]} \quad (1)$$

Table 2. Boundary condition of CFD analysis

Boundary domain	Condition	Value
Inlet	Mass flow rate	Variable [kg/s]
Outlet	Relative pressure	3.5 [bar]
Rod outer	No slip	-
Wire outer	No slip	-
Duct wall	No slip Adiabatic	-
Heat source (clad inner surface)	Function of Z axis	P(z)

2.4 Turbulence model

Three major numerical analysis techniques can be used for turbulent flow fields: direct numerical simulation (DNS), large eddy simulation (LES), and Reynolds-averaged Navier-Stokes (RANS) simulation. RANS uses time-based, ensemble-averaged Navier-Stokes equations and models all of the effects from turbulence. Although RANS yields a lower resolution of analysis than DNS or LES, it is widely used in engineering applications due to the practical aspect of not requiring high-resolution calculation grids. The turbulence models for the RANS equations are for computing the Reynolds stresses tensor from the turbulent fluctuations in the fluid momentum. The turbulence models such as k-ε, k-ω, and SST have become industry standard models and are commonly used for most types of engineering problems. The SST model solves the above problems for switching to the k-ε model in the free-stream and the k-ω model in the viscous sublayer [10]. Sensitivity studies of turbulence models such as Reynolds Stress Model (RSM), k-ε, k-ω and SST were performed on a 127-pin fuel assembly [21]. In that study, the friction factors with the SST model are 1.5–4.5% higher than that with the k-ε model. The friction factor with the SST model is 1.4–1.5% smaller than that with the k-ω model. Because the SST model switches to the k-ε model and the k-ω model, the value of the friction factor with the SST model is between that with the k-ε model and that with the k-ω model. The minimum grid scale on the fuel rod surface was 5.0×10^{-7} mm to capture the laminar to turbulent flow transition with the SST turbulence model the friction velocity y^+ is approximately close to 2.5. In this study, the SST model of CFD was used for investigation.

3. Result

3.1 Code verification

To verify the CFD result in the steady state, it was compared with the MARS-LMR code, which is a system analysis code. MARS-LMR is a code developed to perform DBE (Design Basis Event) transient analysis of SFR (Sodium-Cooled Fast Reactor).

MARS-LMR code is based on MARS code and provides various liquid metal related functions such as sodium heat transfer model, pressure drop model, and reactivity model.

As shown in Table 3, When comparing the system analysis code and the initial condition of the DBE accident under the same conditions, it was confirmed that the peak coolant temperature was the same. Fig. 4 shows the temperature contour at the outlet at a flow rate of $Re = 65,470$, and Fig. 5 shows the normalized outlet average temperature in various Reynolds number ranges. On the wall surface, the power per flow rate of subchannel is small and it has the characteristic of being supercooled compared to the inside.

Table 3. Comparison of initial conditions for transient analysis [8,11]

Parameters	Design Value	MARS-LMR Calculated Value	SAS4A/SASSYS-1 Calculated Value	CFD Value
Core Power [MWt]	392.2	392.2	392.2	392.2
Core flowrate [kg/s]	1984.2	1988.1	1992.95	1984.2
Core inlet temperature [°C]	390	390.12	390.00	390.0
Peak coolant temperature [°C] (FA outlet region)	569.1	568.91	565.9	569.51

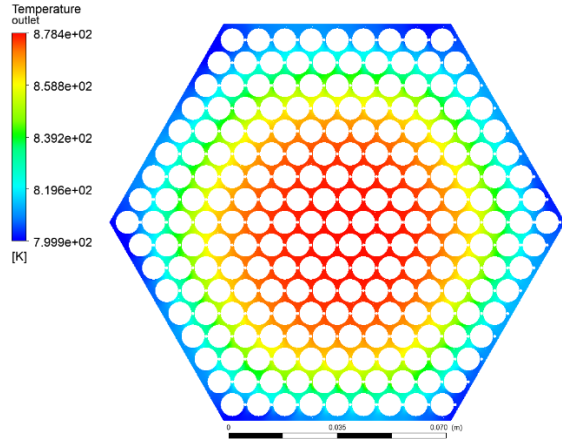


Fig. 4. Outlet temperature contour in Re=65,470

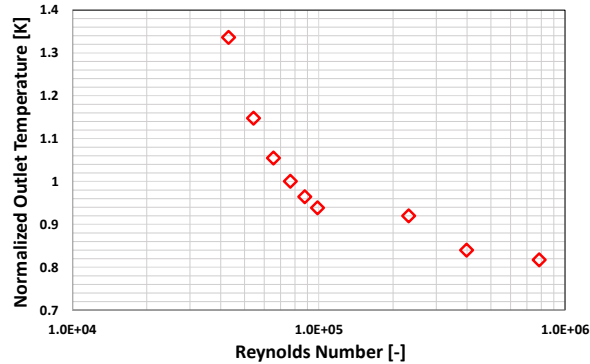


Fig. 5. Outlet Temperature in various range of Reynolds number.

3.2 Pressure drop

Many researchers have conducted experiments to derive the friction factor correlation of wire-wrapped rod bundles. The pressure drop on fully developed flow is calculated as follows:

$$f = \Delta P \frac{D_h}{L} \frac{2}{\rho V^2} \quad (2)$$

Rehme[12], Engel[13], Cheng, and Todreas[14,15] have compared the correlations of the friction factor of fuel assembly in various Reynolds number ranges in detail and evaluated the applicable ranges. Eqs. (3)-(6) show the relational expressions and applicable ranges.

The Rehme(1973) correlation

$$f = \left(\left(\frac{64}{Re} \right) F^{0.5} + \left(\frac{0.0816}{Re^{0.133}} \right) F^{0.9335} \right) (Nr)\pi(D + D_w)/St \quad (3)$$

Where:

$$F = (P/D)^{0.5} + (7.6(P/D)^2 (D + D_w)/H)^{2.16}$$

The Engel(1979) correlation

$$\text{Laminar flow : } f = \frac{110}{Re} \text{ for } Re \leq 400 \quad (4.1)$$

$$\text{Turbulent flow : } f = \frac{0.55}{Re^{0.25}} \text{ for } Re \geq 5000 \quad (4.2)$$

The simplified Cheng and Todreas(1986) correlation

$$\text{Laminar flow : } f = \frac{C_{fL}}{Re} \text{ for } Re \leq Re_L \quad (5.1)$$

$$\text{Turbulent flow : } f = \frac{C_{fT}}{Re^{0.18}} \text{ for } Re_T \leq Re \quad (5.2)$$

Where:

$$Re_L = 300(10^{1.7(P/D-1.0)})$$

$$Re_T = 10,000(10^{0.7(P/D-1.0)})$$

$$C_{fL} = (-974.6 + 1612.0(P/D)$$

$$- 598.5(P/D)^2)(H/D)^{0.06-0.085(P/D)}$$

$$C_{fT} = (0.8063 - 0.9022(\log H/D)) + 0.3526(\log(H/D))^2$$

$$\times (P/D)^{9.7} (H/D)^{1.78-2.0(P/D)}$$

The detailed Upgraded Cheng and Todreas(2018) correlation

$$\text{Laminar flow : } f = \frac{C_{fL}}{Re} \text{ for } Re \leq Re_L \quad (6.1)$$

$$\text{Turbulent flow : } f = \frac{C_{fT}}{Re^{0.18}} \text{ for } Re_T \leq Re \quad (6.2)$$

$$C_{fL} = De_b \left(\sum_{i=1}^3 \left(\frac{N_i A_i}{A_b} \right) \left(\frac{De_i}{De_b} \right) \left(\frac{De_i}{C_{fiL}} \right) \right)^{-1}$$

$$C_{fT} = De_b \left(\sum_{i=1}^3 \left(\frac{N_i A_i}{A_b} \right) \left(\frac{De_i}{De_b} \right)^{0.0989} \left(\frac{De_i}{C_{fiT}} \right)^{0.54945} \right)^{-1.82}$$

where i = b, 1, 2 or 3 for bundle average, interior, edge and corner subchannel.

Fig. 6 shows a comparison of the 217-pin fuel assembly CFD analysis results with the friction factor correlations. In normal operating range, the CFD result was the best fit with the UCTD relational expression. It has been reported that the UCTD relation is the most desirable for the best accuracy of the pressure drop analysis of wire-wrapped fuel rod bundles. [16]

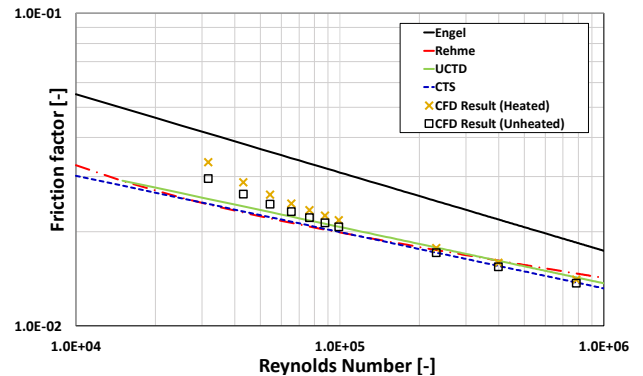


Fig. 6. Friction factor in a wire-wrapped 217-pin fuel assembly

It can be observed from Fig.6 that the friction factor is different when heat flux is applied to the rod (Heated

condition) and when it is not applied (Unheated condition). In the heated condition, an additional pressure drop was caused by the flow acceleration or deceleration by the variation of fluid density. Therefore, a larger coefficient of friction factor appeared when compared to the unheated condition.

3.3 Heat transfer

Thermal energy from fission in the fuel pins is transferred to the coolant by convection. For SFR, the coolant is sodium, which has a higher transfer coefficient than other fluids. For sodium, the Prandtl number is very small, typically in the range of less than 0.01 [17]. This means that the mechanism of conductive heat transfer dominates over the momentum transfer mechanism.

Most turbulence models that use the concept of eddy diffusivity to describe turbulent heat transfer use turbulent Prandtl numbers. Eq. (7) is an equation that determines the Prandtl number (Pr) used in CFD analysis.

$$\mu = \mu_l + \mu_t \quad (7)$$

An eddy viscosity (μ) is calculated by a turbulence model, and then, Prandtl number can be determined by Eq. (8) [18]

$$\frac{\mu}{Pr} = \frac{\mu_l}{Pr_l} + \frac{\mu_t}{Pr_t} \quad (8)$$

As shown in Fig. 7, the CFD analysis result with Prt of 0.02 is compared with the Mikityuk[19], Subbotin[20] and Borishanski[21] models. Eqs. (9)-(11) show the relational expressions and applicable ranges.

The Mikityuk correlation (2009)

$$Nu = 0.047(1 - e^{-3.8(P/D-1)})(Pe^{0.77} + 250) \quad (9)$$

$(1.1 \leq P/D \leq 1.95, 30 \leq Pe \leq 5000)$

The Subbotin correlation (1965)

$$Nu = 0.58 \left(\frac{D_h}{D}\right)^{0.55} Pe^{0.45} \quad (10)$$

$(1.1 \leq P/D \leq 1.5, 80 \leq Pe \leq 4000)$

The Borishanski correlation (1969)

$$Nu = 24.15 \log(-8.12 + 12.76(P/D) - 3.65(P/D)^2) + 0.0174(1 - e^{-6((P/D)-1)})B \quad (11)$$

Where:

$$B = \begin{cases} 0, & Pe < 200 \\ (Pe - 200)^{0.9}, & Pe \geq 200 \end{cases}$$

$(1.1 \leq P/D \leq 1.5, 60 \leq Pe \leq 2200)$

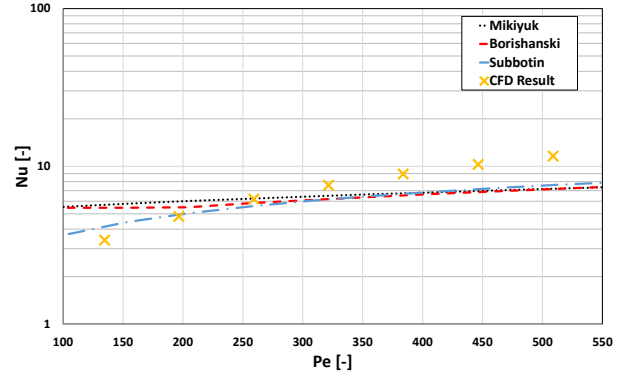


Fig. 7. Heat transfer comparison of correlations and the CFD results

3.4 Vortical flow phenomena

Complicated and vortical flow phenomena in the wire-wrapped fuel bundles have been elucidated by a CFD analysis with a high resolution scheme and a shear stress transport (SST) turbulence model, and by a vortex structure identification technique based on the critical point theory. [22] In this chapter, the vortex structure analysis was conducted to investigate the same aspect as the existing analysis. The vortex structure was well predicted in the case of heat generation.

As shown in Figure 8, the relative position of the vortex in each sub-channel is closely related to the vortex structure behavior and the three-dimensional flow phenomenon. The edge, corner, and interior vortex structures are periodically changed according to the relative positions of the wire-a-spacer and the duct.

Fig. 9 shows, the multi-scale vortex structures are developed in the fuel assembly. The edge vortex structure has a larger axial velocity than other vortexes structure, and the edge vortex structure is a type of longitudinal vortex and has a larger scale than other sub-channels. The strong longitudinal vortex structure in the edge sub-channel can achieve better heat transfer characteristic than in the corner and interior sub-channels. The vortex structure affects the heat transfer characteristics.

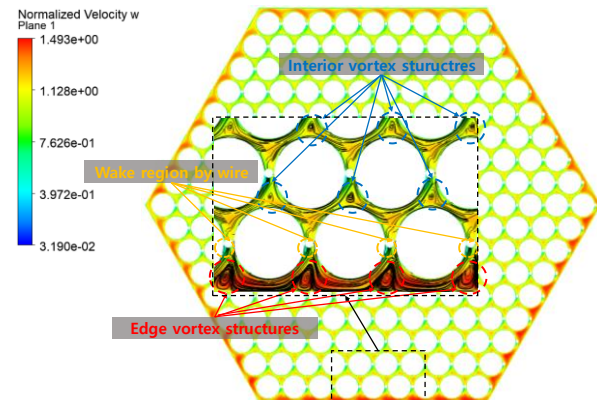


Fig. 8. Normalized axial velocity distribution on the cross sectional planes (Z=440 mm)

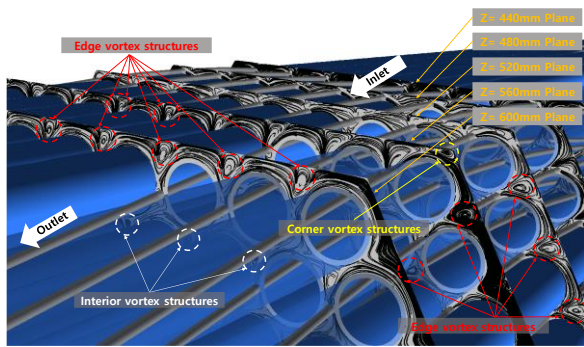


Fig. 9. Projected streamline on the cross sectional planes (Z=440 ~ 600 mm)

4. Conclusion

The thermal-hydraulic phenomena in a 217-pin a wire-wrapped fuel assembly of KAERI PGSFR with the normal operating design value was elucidated with CFD simulation. According to the results of the CFD investigation, the conclusions are as follows:

1. The CFD analysis results have a good agreement with MARS-LMR results. SFRs were compared by outlet temperature due to lack of verifiable data.
2. The friction factor was evaluated in various Reynolds number ranges, and it has very close value with the UCTD correlation.
3. The Nusselt number, was the best fit with the correlation.
4. The validity of the analysis results was analyzed by comparing with the important relational expressions of the fuel assembly.
5. The behaviors of edge, corner, and interior vortex structures are significantly related to the relative positions of wire spacers and ducts.
6. Thermal-hydraulic behaviors such as natural circulation effect in various design basis accidents shall be investigate based on this study.

ACKNOWLEDGMENTS

The research paper was made possible through the encouragement and support from Dr. Su-Jong Yoon of Idaho National Laboratory. This research has been supported by National R&D Program through the National Research Foundation of Korea (NRF) funded by the Ministry of Science, ICT & Future Planning (No. 2021M2E2A208106211).

REFERENCES

[1] M. Naveen Raj, K. Velusamy, "Characterization of velocity and temperature fields in a 217 pin wire wrapped fuel bundle of sodium cooled fast reactor", *Annals of Nuclear Energy*, vol.87, pp.331-349, 2016.

[2] Jing Chen, Dalin Zhang, Ping Song, Xinan Wang, Shibao Wang, Yu Liang, Suizheng Qiu, Yapei Zhang, Mingjun Wang, G.H. Su, "CFD investigation on thermal-hydraulic behaviors of a wire-wrapped fuel subassembly for sodium-cooled fast reactor", *Annals of Nuclear Energy*, vol. 113, pp.256-269, 2018.

[3] Sun Rock Choi, Jae-Yong Lim, Jong Hyuck Won, June-Hyung Kim, Jin-Sik Cheon, "Thermo-mechanical behavior of all the metallic fuel rods in a sodium-cooled fast reactor", *Nuclear Engineering and Design*, vol. 339, pp.126-136, 2018.

[4] Jae-Ho Jeong, Min-Seop Song, Kwi-Lim Lee, "RANS based CFD methodology for a real scale 217-pin wire-wrapped fuel assembly of KAERI PGSFR", *Nuclear Engineering and Design*, vol. 313, pp.,470-485, 2017.

[5] Gajapathy, R., Velusamy, K., Selvaraj, P., et al. "CFD investigation of effect of helical wire-wrap parameters on the thermal hydraulic performance of 217 fuel pin bundle", *Annals of Nuclear Energy*, vol. 77, pp. 498–513, 2015.

[6] Pointer, W.D., Thomas, J., Fanning, T., Fischer, P., Siegel, A., Smith, J., Tokuhira, A. "RANS-based CFD Simulation of Sodium Fast Reactor Wire-wrapped Pin Bundles.", M&C, Saratoga Springs, USA, 2009.

[7] Yamamoto, K., "An Elliptic-hyperbolic Grid Generation Method and Application to Compressor Flows.", *Special Publication of National Aerospace laboratory*, SP 19, pp. 193-198, 1992.

[8] Choi, S.R. *Dimensions of PGSFR Fuel Assembly*. KAERI. SFR-IOC-R/M-14-003, 2014.

[9] Sun Rock Choi, "PGSFR 노심 열수력 설계 방법론", KINS 원자력안전심포지엄, 2019.

[10] Menter, F.R. "Two-equation eddy-viscosity turbulence models for engineering applications.", *AIAA J.* vol. 32 (8), pp. 1598–1605, 1994.

[11] JH Jeong, "소듐냉각고속로 계통과도안전해석 MARS-LMR 전산코드 검증", KINS 원자력안전심포지엄, 2019

[12] K. Rehme, "Pressure Drop Correlations for Fuel Element Spacers," *Nuclear Technology*, vol. 17, pp. 15-23, 1973.

[13] F. Engel, R. Markley and A. Bishop, "Laminar, Transition, and Turbulent Parallel Flow Pressure Drop Across Wire-Wrap-Spaced Rod Bundles," *Nuclear Science and Engineering*, vol. 69, no. 2, pp. 290-296, 1979.

[14] Cheng, S.K., Todreas, N.E., "Hydrodynamic models and correlations for bare and wire-wrapped hexagonal rod bundles – bundle friction factors, sub-channel friction factors and mixing parameters." *Nuclear Engineering and Design*, vol. 92, pp.227-251, 1986.

[15] S.K. Chena, Y.M. Chena, N.E. Todreas, "The upgraded Cheng and Todreas correlation for pressure drop in hexagonal wire-wrapped rod bundles", *Nuclear Engineering and Design*, vol. 335, pp.356-373, 2018.

[16] Su-Jong Yoon, Florent Heidet, "Evaluation of Pressure Drop Correlations for the Wire-wrapped Rod Bundles", ANS, vol. 122, pp.803-806, 2020.

[17] Waltar, A.E., Reynolds, A.B., 1980. Fast Breeder Reactors. Pergamon Press.

[18] Jae-Ho Jeong, Min-Seop Song, Kwi-Lim Lee, "Thermal-hydraulic effect of wire spacer in a wire-wrapped fuel bundles for SFR", Nuclear Engineering and Design, vol. 320, pp.28-43

[19] Konstantin Mikiyuk, "Heat transfer to liquid metal: Review of data and correlations for tube bundles", Nuclear Engineering and Design, vol. 239, pp.680-687, 2009.

[20] Subbotin, V.I., Ushakov, P.A., Kirillov, P.L., Ibragimov, M.H., Ivanovski, M.N., Nomofilov, E.M., Ovechkin, D.M., Sorokin, L.N., Sorokin, V.P., Heat transfer in elements of reactors with a liquid metal coolant. In: Proceedings of the 3rd International Conference on Peaceful Use of Nuclear Energy, 8, NY, pp. 192-200, 1965.

[21] Borishanski, V.M., Gotovski, M.A., Firsova, E.V., "Heat transfer to liquid metals in longitudinally wetted bundles of rods", Soviet Atomic Energy, vol. 27, pp. 1347-1350, 1969.

[22] Jae-Ho Jeong, Min-Seop Song, Kwi-Lim Lee, "CFD investigation of three-dimensional flow phenomena in a JAEA 127-pin wire-wrapped fuel assembly", Nuclear Engineering and Design, vol. 323, pp.166-184, 2017.